Title: Natural evolution of SARS-CoV-2 variants in K18-ACE2 mice gives rise to more virulent virus and variant alleles associated with treatment resistance.

Authors: Julian Daniel Sunday Willett[1,2,3], Annie Gravel[4], Isabelle Dubuc[4], Leslie Gudimard[4], Paul Fortin[4,5,6], Ju-Ling Liu[2,8], Jose Hector Galvez[7], Melissa Zwaig[2,8], Anne-Marie Roy[2,8], Sally Lee[2,8], Shu-Huang Chen[2,8],Jiannis Ragoussis[2,8]*, Louis Flamand[4,9]*

Affiliations:

1. Quantitative Life Sciences Ph.D. Program, McGill University, Montreal, QC, Canada
2. McGill University Genome Centre, Montreal, QC, Canada
3. Lady Davis Institute, Jewish General Hospital, Montreal, QC, Canada
4. Axe maladies infectieuses et immunitaires, Centre de Recherche du Centre Hospitalier Universitaire de Québec- Université Laval, Canada
5. Centre de Recherche ARThrite-Arthrite, Recherche et Traitements, Université Laval, Québec, QC, Canada.
6. Division of Rheumatology, Department of Medicine, CHU de Québec-Université Laval, Québec, QC, Canada
7. Canadian Centre for Computational Genomics, McGill University, Montreal, QC, Canada
8. Department of Human Genetics, McGill University, Montreal, QC, Canada
9. Département de microbiologie-infectiologie et d'immunologie, Université Laval, QC, Canada.

*Co-corresponding authors

Abstract:

Background: The continuing COVID-19 pandemic is partially due to viral evolution decreasing vaccine and treatment efficacies. Predicting viral evolution is difficult. Others have found that serial infections of the original SARS-CoV-2 isolate in non transgenic mice is accompanied with selection of alleles (such as Spike 417N, 493H and 501Y) conferring adaptation and greater binding affinity for the murine ACE2 receptor, enhanced infectivity, and lethal phenotype in mice. We designed a study to investigate long-term viral evolution's impact in K18-ACE2 mice with virus closer related to the Omicron sub-lineage.

Methods: We serially infected SARS-CoV-2-naïve mice with either the B.1.351 (Beta) or the B.1.617.2 (Delta) variant across twenty passages without selective pressures. We sequenced virus across passages, annotating variant alleles changing in frequency using published tools, tracking alleles suspected of decreasing vaccine/treatment efficacy. We evaluated virulence in animals infected with virus isolated at study completion and determined antibody neutralization sensitivity using sera from vaccinated individuals.

Results and Conclusions: We observed variant alleles with documented roles in vaccine-elicited immunity evasion. This included the Omicron-associated mutation spike S371F that arose *de-novo* during our study. Passage 20 (P20) viruses were more virulent that their P0 counterpart with P20 Delta lineage being significantly more resistant to antibody neutralization. These developments occurred within two months of the study starting, suggesting that our model can rapidly emulate pandemic progression in mammals. While our model lacked selective pressures, such as pre-existing SARS-CoV-2 immunity, these conditions could readily be adapted. Such modeling could enable development of more evolution-resistant treatments.

Keywords: SARS-CoV-2, COVID-19, pandemic modelling, treatment resistance, viral evolution.

Background:

Part of the difficulty in responding to COVID-19 has been predicting viral evolution and its impact on clinically relevant traits, such as infectivity, treatment resistance, and disease severity (1). The basic biology of the severe acute respiratory syndrome Coronavirus 2 (SARS-CoV-2), the virus that causes COVID-19, is well understood. However, our knowledge of SARS-CoV-2 evolution is limited. Many RNA viruses, such as SARS-CoV-2, exist as quasi-species meaning that within a given viral population, a multitude of alleles (major and minor) are constantly present. These alleles give plasticity to the viral population allowing for rapid adaptation/selection to a variety of circumstances (2). Viral evolution is also complex and affected by several factors, including host genetic background (3), host immune status (4), the organs targeted by the virus (5), and a population's collective immunity (6). As a result, it has been difficult to predict the emergence of new variants with altered virulence.

Several variants of concern (VOC) have emerged, each with mutations providing dissemination advantages (1). For example, the SARS-CoV-2 alpha variant (B.1.1.7) gained a growth advantage and rapidly spread globally due to the spike protein N501Y mutation that enhances affinity for the cellular entry receptor, angiotensin-converting enzyme 2 (ACE2) (7). Other VOC, such as the Delta (B.1.617.2) variant, gained advantages with additional substitutions in spike, including L452R (8), T478K (9), and P681R (10) that affect viral transmissibility and antibody neutralization for naturally or artificially vaccinated individuals (11). To better predict changes in SARS-CoV-2 and reduce the impact of a future pandemic, time effective models must be defined for studying viral changes over successive generations.

In 2020, Gu *et al.* studied short-term viral evolution by infecting aged mice with the SARS-CoV-2 reference strain (IME-BJ05) and collecting lung tissue at set timepoints following infection, using this isolate to infect successive generations of mice (12). While wild-type mice are thought less

susceptible to the virus as mouse ACE2 is not used by SARS-CoV-2 as its receptor, Gu *et al.* demonstrated that serial passaging of lung homogenate across mice produced a mouse-adapted strain (MASCp6) that causes pulmonary symptoms, matching adaptations observed by others who previously applied the technique to influenza (12, 13). After six passages, they found several clinically relevant genetic changes, including de-novo appearance of A23063T that changes spike to N501Y (12). This mutation is associated with enhanced viral infection and transmission (7). Subsequently, the group passaged the MASCp6 isolate an additional 30 times and characterized the MASCp36 isolate (14). MASCp36 contained several mutations (i.e. K417N, Q493H and N501Y mutations) in spike conferring greater ACE2 receptor binding affinity, increased infectivity and greater virulence (14). Others replicated this study using the same viral variant, observing similar development of clinically relevant variant alleles (15).

Since these studies, new lineages arisen, with the present being Omicron, negatively impacting treatment efficacy (1). Others have studied viral dynamics using recent lineages in serial passages in cells, observing similar development of directional selection and clinically concerning mutations (16, 17). Given the pandemic's prolonged nature, understanding longitudinal viral changes in a mammalian host is pressing. We adapted Gu *et al.*'s approach to evaluate how viral lineages more closely related to the present lineages, B.1.351 (Beta) and B.1.617.2 (Delta), changed over twenty passages (12). Given clinically relevant mutations arising in Gu *et al.*'s studies (12, 14), we sought to determine if impactful variant alleles would develop in more recent viral variants. We report on the *de novo* appearance and persistence of variant alleles associated with treatment resistance with serially passaged virus demonstrating increased viral virulence and antibody resistance.

Methods:

Viruses. SARS-CoV-2 Wuhan-like strain (LSPQ, B1 lineage) was obtained from the Laboratoire de Santé Publique du Québec ([LSPQ] Sainte-Anne-de-Bellevue, QC, Canada). SARS-CoV-2 Beta strain was obtained from BEI resources and SARS-CoV-2 Delta strain from the BC Centers for Disease Control. SARS-CoV-2 strains were propagated on Vero cells (American Type Culture Collection, Manassas, Virginia, USA).

***Determination of the viral titer*.** Vero cells were plated in a 96-well plate ($2x10^4$/well) and infected with 200µl of serial dilution of the viral preparation or lung homogenate in the M199 media supplemented with 10mM HEPES pH 7.2, 1mM of sodium pyruvate, 2.5g/L of glucose, 5µg/mL *Plasmocin*® and 2% FBS. Three days post-infection plates were analyzed using a EVOS M5000 microscope (ThermoFisher Scientific, Waltham, MA, USA) and the viral titer was determined using the Karber method (18).

Mouse models. B6.Cg-Tg(K18-hACE2)2Prlmn/J (stock#3034860) and B6 mice were purchased from the Jackson Laboratories (Bar Harbor, ME). One K18-ACE2 mouse was intranasally infected with either B.1.351 (Beta) or B.1.617.2 (Delta) SARS-CoV-2 lineages. Following 3-4 days, the animals were sacrificed and lung homogenate collected. The homogenate was used to intranasally infect sequential animals, defined as passage. This was repeated for 10 passages. After passage 10 (P10), virus in lung homogenate was sequenced. K18-ACE2 mice were then intranasally infected with Beta P10 or Delta P10 with viruses passaged in three mice at a time for an additional 10 times (total of 20 passages) with virus in lung homogenate sequenced following passages 13, 17, and 20 (**Figure 1**). Viral stocks were then made from lung homogenates of Beta and Delta P20 viruses. K18-ACE2 mice were infected intranasally with 500 $TCID_{50}$ of P0 or P20 viruses. Lung viral loads were determined on day 3 post-infection with weight loss and survival monitored daily for up to 9 days.

Infectivity of P0 and P20 viruses to non-transgenic mice. C57BL6 mice were infected intranasally with 3000 $TCID_{50}$ of P0 and P20 Beta and Delta viruses. Three days later, mice were euthanized, and lungs collected for viral load (titer) determination.

RNA extraction: Up to 30 mg of lung tissue were used for RNA extraction using the Bead Mill Tissue RNA Purification Kit and the Bead Mill Homogenizer, following manufacturer's instructions.

Viral sequencing. RNA extracts were processed for reverse transcription (step a) and targeted SARS-CoV-2 amplification using the ARTIC V3 or V4.1 primer scheme (https://github.com/artic-network/primer-schemes/tree/master/nCoV-2019) (step b). Samples were purified (step b) and Nextera DNA Flex library preparation (step c) was performed for Illumina PE150 paired-end amplicon sequencing on a NovaSeq or MiSeq instrument at the McGill Genome Centre using best practices. Each sample was sequenced twice on different days to obtain a target of minimum 10 million reads per sample. The detailed protocols can be accessed with the following links.

Step a: dx.doi.org/10.17504/protocols.io.bjgekjte.

Step b: dx.doi.org/10.17504/protocols.io.ewov18e4ygr2/v2.

Step c: dx.doi.org/10.17504/protocols.io.bjgnkjve.

***Genome data processing*.** Following sequencing, the reads from each sample were used to call variants using Freebayes v1.3.6 (19) and the results were saved as a VCF file which was used to compare genomic variation across passages. The process is described briefly as follows: first, the raw reads from each sample were aligned with BWA MEM v0.7.17 (20) to the reference strain genome sequence (NC_045512.2). The resulting alignments were sorted with

duplicate reads flagged. The minimum number of aligned reads for each was logged, and each sample was again aligned and processed, then randomly down sampled to match this minimum number of reads. All variants with a quality of less than 20 or a depth below 10 were removed from the analysis. Any variant alleles that overlapped with ARTIC sequencing primers were also removed. Merged VCF files, representing the combination of reads across two sequencing batches for each sample, were used for the paper's main results.

Variant annotation. Every variant allele was inputted into COVID-19 Ensembl variant effect predictor (VEP) (https://covid-19.ensembl.org/index.html) to determine functional consequences and the involved gene and amino acid change (21). Variants whose VAF changed at least once across passages during the study were logged and input to the UCSC Genome Browser (https://genome.ucsc.edu/), checking for annotations of antibody escape, CD8 escape, vaccine targets, drug resistance, or variants of concern (22).

Antibody neutralization studies. Sera from three, healthy vaccinated individuals (ERB #2022-6204) were analyzed for neutralizing activity against Wuhan-like, and Beta and Delta P0 and P20 viruses (n = 12). Serially diluted sera (in quadruplicate) were incubated with 100 $TCID_{50}$ of virus for 1 h at 37˚C before addition to Vero E6 cells. Three days later, the 96-well plates were observed using an inverted microscope for signs of infection. Neutralization titers were determined and defined as the highest serum dilution preventing infection.

Ethics. The study was conducted in accordance with the Declaration of Helsinki, and mouse protocols were approved by the Comité de protection des animaux de l'Université Laval.

Statistics. All statistical analyses were conducted using R/4.2.1. All statistical comparisons between passages were corrected for multiple testing using a Benjamini-Hochberg p-value adjustment.

Source code. All code used in this study, from sample processing to data analysis, are publicly available on Github at the following link: https://github.com/juliandwillett/SARS_CoV_2_Serial_Passaging_Study.

Data availability. VCF files used to complete computational analyses are available by reasonable request.

Funding. This study was supported by the Canadian Institutes for Health Research (CIHR 476575) operating grant to the Coronavirus Variants Rapid Response Network (CoVaRR-Net) to LF and IR and CIHR grant (GA1-117694) to LF.

Results:

Variant allele frequency of alleles across passages. The minimum number of reads per sample across P13, P17, and P20 was 34,253,784. In Beta lineage, there was a significantly lower variant allele frequency (VAF) in P17 and P20 versus other passages (adjusted p-value < 0.05), with a significant difference in Delta comparing P10 and P20 (**Figure 2a-b**). As there was no significant change in allele depth across the study, these VAF differences could be due to growing allelic diversity. Such significant changes, less consistent with random allelic drift, could align with suggested mechanisms of within-host evolution of the variant allele pool, per Tonkin-Hill *et al*. (23). Sample contamination is less likely as there was no significant difference in VAF or variant allele depth between samples for either viral lineage (**Figure 2c-d**).

Gene involvement and variant allele functional consequence severity did not significantly vary across passages. There was no statistically significant change in the proportion of variant alleles involving a specific gene or severity of variant allele predicted functional consequence across the study (adjusted p-value > 0.05) (**Figure 3**), suggesting that the overall allele population did not significantly change in our model without imposed selective pressures (6).

Development of variant alleles associated with clinically relevant traits. We observed 82 unique variant alleles across our study. There were 41 whose VAF changed with 32 having clinically-relevant annotations, including interactions with human proteins, mutations that may confer drug resistance, variant alleles associated with the Omicron lineage, mutations associated with antibody escape, and mutations at vaccine targets (**Table 1, Supplemental Table 1**) (22, 24). A notable novel variant included C22674T, or Spike S371F, that arose *de-novo* in two animals in P20 for Beta virus and two animals in P13 for Delta virus (**Figure 4**). The allele is associated with protein interactions, antibody escape, affects a vaccine target, and is an Omicron-specific mutation (**Table 1**) (22, 25). We thus observed an Omicron specific mutation in a study not involving Omicron viral lineages. Several other variants changing in frequency also conferred possible drug resistance and targeted the vaccine site (**Table 1**) (22).

Most alleles in the P0 Beta isolate, passaged several times *in vitro* in Vero cells, encoded a Spike protein with a tryptophan (W) at position 682 (C23606T), destroying the furin cleavage site (**Table 1**). We observed a rapid selection of viruses having the reference allele encoding an arginine (R) at position 682 and functional furin site in all animals infected with Beta variant starting in P10 (**Table 1**). This suggests that the furin site provides a growth advantage under *in vivo* conditions and supports a previous report indicating the Spike furin site being important for SARS-CoV-2 virulence in K18-ACE2 mice (26).

Later passage virus was linked with greater weight loss, virus producing larger viral loads more quickly, and reduced antibody neutralization. Unlike Gu *et al*.'s study that required adaptation of SARS-CoV-2 to a murine ACE2 receptor for infectivity, our study made use of transgenic mice expressing the human ACE2 receptor (12). We determined whether repeated passaging of SARS-CoV-2 in K18-ACE2 mice affected virulence by infecting animals with P0 and P20 viruses with clinical scores and viral loads determined. On day 3 post-infection, no differences in viral load were noted between Beta P0 and Beta P20 viruses with mice infected with P20 Delta virus

having a significant increase (6.3x) in lung viral loads (**Figure 5A**). Both P20 Beta and P20 Delta viruses caused more rapid and greater weight loss than P0 viruses (**Figures 5B-C**) with similar survival curves (**data not shown**).

We then assessed whether repeated passages in K18-ACE2 mice would result in viruses capable of infecting non transgenic mice. C57BL6 mice were infected intranasally with P0 and P20 viruses and lung infectious viral loads determined 3 days later. Both P0 and P20 Beta viruses successfully replicated in mouse lungs with both viruses producing similar viral loads (**Supplementary Figure 2**). None of the P0 or the P20 Delta viruses generated viral loads in lungs of B6 mice (**Supplementary Figure 2**).

Our results indicate that Delta P20 viruses generate a greater viral load that P0. To determine if this was related to growth kinetic differences between P0 and P20 viruses, we performed *in vitro* growth curve analysis. We observed two independently evolved P20 Delta viruses replicating more efficiently after 24 h versus P0, yielding 4-5X more infectious virus after 24h of infection (**Figure 6**). This difference in viral titers was no longer observed after 48 h (**Figure 6**).

We next determined the ability of sera from vaccinated subjects to neutralize passaged viruses, comparing it to parental P0 viruses. Consistent with previous reports, sera from vaccinated subjects had varied neutralizing potential depending on the variant, with neutralization titers being greatest against the original Wuhan-like strain and lowest for the Beta isolate (**Figure 7A**) (27, 28). The same sera were analyzed for their ability to neutralize P20 viruses. P20 Beta was neutralized equally (8 out of 12) or more efficiently (4 of 12) that the P0 virus (**Figure 7B**). In contrast, P20 Delta virus was significantly less sensitive to antibody neutralization by vaccinated subject sera than P0 ($p < 0.05$) where 7 of 12 sera showed decreased neutralizing potential toward the P20 Delta virus relative to P0 (**Figure 7C**).

Discussion:

In this study, we serially infected mice with Beta or Delta lineage virus for twenty passages without selective pressures. The evolved viruses developed and maintained variant alleles associated with treatment resistance and later lineages like Omicron (**Figure 4, Table 1**), were more virulent (**Figure 5**), grew faster and to higher levels (Delta) (**Figure 6**) and were less sensitive to antibody neutralization (Delta) (**Figure 7**), demonstrating immune escape potential. These developments occurred within roughly two months, illustrating the model's potential in rapidly emulating pandemic progression that could facilitate treatment/vaccine development less sensitive to viral evolution. The model can readily be adapted to mimic viral adaptation in the context of immune or anti-viral selection pressures, affording rapid results in a system often seen in real world conditions.

Our model lacked selective pressures, mimicking the evolution of SARS-CoV-2 in a naïve population. Using K18-ACE2 transgenic mice eliminated the selective pressure of adapting virus to the murine ACE2 receptor. The Beta P0 virus harbored the N501Y mutation previously reported to enable adaptation of reference SARS-CoV-2 in non transgenic mice (12). This mutation was maintained throughout passages, suggesting that this virus can infect cells through the murine ACE2 receptor as well (**Figure 4**). Our data supports this, as non transgenic C57BL6 mice were equally susceptible to infection by Beta P0 and P20 viruses. This capacity of Beta to use human and murine receptors might explain, at least in part, the greater virulence of the Beta isolate in ACE2 transgenic mice relative to other viral isolates, such as Wuhan and Delta lacking the N501Y mutation in transgenic mouse studies (29).

The Delta P0 virus lacked the N501Y mutation and never acquired it following repeated passages in ACE2 transgenic mice. This highlights that when lacking selective pressure, such as neutralizing antibodies, the appearance of N501Y is not favored (**Figure 4**). Acquisition of

N501Y in the human population was first reported almost a year after the initial report of the SARS-CoV-2 epidemic, suggesting that this mutation arose during the development of herd immunity (30).

Of the 41 variant alleles that arose *de-novo* or changed in frequency during the study, several are of clinical interest (**Figure 4, Table 1**). A4981G, which arose *de-novo* and persisted in Beta lineage virus in P17 (**Figure 4**), was predicted to possibly confer drug resistance to papain-like protease inhibitors (31), such as ritonavir used clinically in combination with nirmatrelvir that protects patients against severe COVID-19 (32, 33). C22674T, or spike S371F, which arose *de-novo* and persisted in two animals in P20 for Beta and P13 for Delta virus (**Figure 4**), represents an Omicron-specific mutation arising in a study that did not use Omicron. This last mutation has been previously reported to facilitate antibody escape (**Table 1**) (25). Considering that the mutation S371F is reported to bear a significant fitness cost (34), this might explain why isolated S371L/F mutations are not viable or have not yet been detected in isolation. We would argue that mutations of residues E484 present in Delta and K417/E484/N501 present in Beta Spike proteins, also found together with the S371F mutation in Omicron BA.2, represent such compensatory mutations. G23593T, or spike Q677H, which disappeared from Beta virus samples after P0, has been determined to enhance treatment resistance and increase viral infectivity (35). The reversion of Spike amino acid 677 to Q after passage in mice could explain the increased neutralization activity for some of the sera against Beta P20 relative to P0 (**Figure 7**). Variants that could impair treatment efficacy appeared and disappeared in this study, showcasing the model's potential in evaluating diverse variants.

This study has limitations. Here we used the K18-ACE2 transgenic mice but the mechanisms of new viral variants arising in humans could significantly differ. This is relevant as host factors are believed to contribute to viral variant allele diversity (36). Our model lacked discernible selective pressures, while the COVID-19 pandemic has been accompanied by contact limitations and

vaccines with the dominant SARS-CoV-2 evolutionary mechanism believed to be natural selection (6). Development or dominance of new variants likely varies with these pressures, necessitating reproducing this model with them. However, a baseline comparison model is required to get the most from these supplemental models, hence the relevance of our model. We studied Beta and Delta lineage virus, which are no longer dominant. Patterns of genetic changes observed in these lineages could vary from Omicron. There was no statistical change in the variant allele population's involvement of specific genes or predicted functional consequence when comparing Beta and Delta lineages across passages, which is reassuring for generalizability.

Conclusions:

The model presented rapidly emulated pandemic progression in a naïve population, with virus accumulating variant alleles that could limit therapies for severe disease, becoming more virulent, and ultimately becoming treatment resistant. These results support that serial viral passaging in mice is a useful method to rapidly study viral evolution enabling development of targeted anti-viral therapies.

List of abbreviations:

ACE2: angiotensin-converting enzyme 2

CIHR: Canadian Institutes for Health Research

CoVaRR-Net: Coronavirus Variants Rapid Response Network

SARS-CoV-2: severe acute respiratory syndrome Coronavirus 2

$TCID_{50}$: 50% tissue culture infectious dose

VAF: variant allele frequency

VEP: variant effect predictor

VOC: variants of concern

Figure Titles and Legends.

Figure 1. **Study design**. First, SARS-CoV-2 ACE2-adapted mice were inoculated with either B.1.351 (Beta) or B.1.617.2 (Delta) virus and left for three days for virus to proliferate. They were then sacrificed with the lung homogenate used to infect another mouse. This was repeated for ten passages. Second, P10 virus for each lineage was used to infect three additional mice and the process was repeated for an additional ten passages. Third, P0 and P20 virus for each lineage was used to infect additional mice to compare weight loss and survival between early and late passage virus, and test non-adapted mouse susceptibility to the virus. Antibody neutralization of virus was also compared.

Figure 2. Boxplots of variant allele frequency by (a-b) passage and (c-d) sample. Each N refers to the number of variant alleles for each MAF and in total. Box fill in (c-d) signifies sample number. For significance, n.s.: adjusted p-value > 0.05, *: adjusted p-value > 0.01, **: adjusted p-value ≤ 0.01.

Figure 3. **Gene involvement and predicted variant allele functional consequence severity (VEP) in variant allele population did not significantly change (adjusted p-value > 0.05) with passage.**

Figure 4. Variants of clinical relevance arose de novo and grew to dominance. VAF: variant allele frequency. P refers to passage.

Table 1. Annotations of select variants that changed in frequency across the study.

Figure 5. Pathogenesis of P0 and P20 viruses in K18-ACE2 mice. Mice (n = 15/group) were infected with 500 $TCID_{50}$ of P0 or P20 Beta and Delta viruses. (A) On day 3 post-infection, mice (n = 5) were euthanized and lungs collected for infectious viral load determination. Results are expressed as mean ± SD SARS-CoV-2 $TCID_{50}$/mg of lung tissue. (B-C) The weight of each mouse (n = 10/group) was monitored daily throughout the experiment and reported as mean percentage ± SD of weight relative to day 0. **: $p \leq 0.008$ as determined using non-parametric Mann-Whitney test.

Figure 6. **Growth kinetics of P0 and P20 Delta viruses**. P0 and two independently evolved P20 Delta viruses were used to infect Vero cells at a multiplicity of infection of 0.005. Cell-free supernatants were collected at 24 h and 48 h and used for viral titration. Results are expressed as mean ± SD $TCID_{50}$/mL. *: p=0.02 as determined using an unpaired t-test.

Figure 7. Neutralization of P0 and P20 viruses with sera from vaccinated subjects. (A) Neutralization assay of Wuhan-like, Beta, and Delta viruses using sera from three vaccinated subjects. Individual results and mean ± SD neutralization titer against different SARS-CoV-2 isolates are presented. ****: $p<0.0001$ and **: p=0.0012 determined using one way-ANOVA. ns: not statistically significant. (B) Pair-wise comparison of the sera used in A in neutralization assay against P0 and P20 Beta viruses. (C) Pair-wise comparison of the sera used in A in neutralization assay against P0 and P20 Delta viruses. *: p=0.017 determined using paired t-test.

Supplemental Table 1. Table of variant alleles that changed MAF during the study. Available in "Supplemental Tables.csv".

Supplemental Figure 1. Viral load comparison between P0 and P20 virus in K18-ACE2 mice.

Supplementary Figure 2. Infection of C57BL6 mice with P0 and P20 Beta and Delta viruses. Mice (n = 5/group) were infected intranasally with 3000 $TCID_{50}$ of P0 or three independently evolved Beta P20 or two independently evolved Delta viruses. On the third day post infection, mice were euthanized and lungs collected for infectious viral load determination. Individual results and mean ± SD $TCID_{50}$/mg of lung tissue are presented.

Declarations:

Ethics approval and consent to participate. The study was conducted in accordance with the Declaration of Helsinki, and mouse protocols were approved by the Comité de protection des animaux de l'Université Laval.

Consent for publication: All authors have consented to publication.

Availability of data and materials. VCF files used to complete computational analyses are available by reasonable request, code is publicly available on Github (refer to Methods), physical materials used are referred to by their product codes.

Competing interest.

All authors declare no competing interests.

Funding. This study was supported by the Canadian Institutes for Health Research (CIHR 476575) to JDSW, and an operating grant to the Coronavirus Variants Rapid Response Network (CoVaRR-Net) to LF and IR and CIHR grant (GA1-117694) to LF. The funding body had no role in the design of the study or collection, analysis, interpretation, or reporting of the data.

Authors contributions. Julian Daniel Sunday Willett conceived of the computational analyses needed for this study, completed all computational analysis of viral sequencing data, and wrote the majority of the manuscript. Louis Flamand and Jiannis Ragoussis conceived of the study.

Louis Flamand contributed to manuscript revisions, wrote sections relevant to animal models and antibody neutralization studies and performed analysis of results. Isabelle Dubuc and Leslie Gudimard performed all works involving live SARS-CoV-2 viruses. Annie Gravel participated in the sequence analysis and methodological design of experiments. Paul Fortin and Ines Colmegna provided key reagents. Jose Hector Galvez contributed bioinformatics analysis review and manuscript revisions. Ju-Ling Liu, Anne-Marie Roy, Sally Lee and Shu-Huang Chen supported the SARS-CoV-2 viral sequencing.

Acknowledgments.

This research was enabled in part by support provided by Calcul Québec (calculquebec.ca) and the Digital Research Alliance of Canada (alliancecan.ca). This work was made possible by funding from the CIHR. We thank Ines Colmegna for providing vaccinated patient sera.

References:

1. Jacobs JL, Haidar G, Mellors JW. COVID-19: Challenges of Viral Variants. Annu Rev Med. 2022.
2. Sun F, Wang X, Tan S, Dan Y, Lu Y, Zhang J, et al. SARS-CoV-2 Quasispecies Provides an Advantage Mutation Pool for the Epidemic Variants. Microbiol Spectr. 2021;9(1):e0026121.
3. Velavan TP, Pallerla SR, Ruter J, Augustin Y, Kremsner PG, Krishna S, et al. Host genetic factors determining COVID-19 susceptibility and severity. EBioMedicine. 2021;72:103629.
4. Belsky JA, Tullius BP, Lamb MG, Sayegh R, Stanek JR, Auletta JJ. COVID-19 in immunocompromised patients: A systematic review of cancer, hematopoietic cell and solid organ transplant patients. J Infect. 2021;82(3):329-38.

5. Van Cleemput J, van Snippenberg W, Lambrechts L, Dendooven A, D'Onofrio V, Couck L, et al. Organ-specific genome diversity of replication-competent SARS-CoV-2. Nat Commun. 2021;12(1):6612.

6. Wang R, Chen J, Wei GW. Mechanisms of SARS-CoV-2 Evolution Revealing Vaccine-Resistant Mutations in Europe and America. J Phys Chem Lett. 2021;12(49):11850-7.

7. Liu Y, Liu J, Plante KS, Plante JA, Xie X, Zhang X, et al. The N501Y spike substitution enhances SARS-CoV-2 infection and transmission. Nature. 2022;602(7896):294-9.

8. Motozono C, Toyoda M, Zahradnik J, Saito A, Nasser H, Tan TS, et al. SARS-CoV-2 spike L452R variant evades cellular immunity and increases infectivity. Cell Host Microbe. 2021;29(7):1124-36 e11.

9. Cherian S, Potdar V, Jadhav S, Yadav P, Gupta N, Das M, et al. SARS-CoV-2 Spike Mutations, L452R, T478K, E484Q and P681R, in the Second Wave of COVID-19 in Maharashtra, India. Microorganisms. 2021;9(7).

10. Liu Y, Liu J, Johnson BA, Xia H, Ku Z, Schindewolf C, et al. Delta spike P681R mutation enhances SARS-CoV-2 fitness over Alpha variant. Cell Rep. 2022;39(7):110829.

11. Planas D, Veyer D, Baidaliuk A, Staropoli I, Guivel-Benhassine F, Rajah MM, et al. Reduced sensitivity of SARS-CoV-2 variant Delta to antibody neutralization. Nature. 2021;596(7871):276-80.

12. Gu H, Chen Q, Yang G, He L, Fan H, Deng YQ, et al. Adaptation of SARS-CoV-2 in BALB/c mice for testing vaccine efficacy. Science. 2020;369(6511):1603-7.

13. Wasik BR, Voorhees IEH, Barnard KN, Alford-Lawrence BK, Weichert WS, Hood G, et al. Influenza Viruses in Mice: Deep Sequencing Analysis of Serial Passage and Effects of Sialic Acid Structural Variation. J Virol. 2019;93(23).

14. Sun S, Gu H, Cao L, Chen Q, Ye Q, Yang G, et al. Characterization and structural basis of a lethal mouse-adapted SARS-CoV-2. Nat Commun. 2021;12(1):5654.

15. Huang K, Zhang Y, Hui X, Zhao Y, Gong W, Wang T, et al. Q493K and Q498H substitutions in Spike promote adaptation of SARS-CoV-2 in mice. EBioMedicine. 2021;67:103381.

16. Chung H, Noh JY, Koo BS, Hong JJ, Kim HK. SARS-CoV-2 mutations acquired during serial passage in human cell lines are consistent with several of those found in recent natural SARS-CoV-2 variants. Comput Struct Biotechnol J. 2022;20:1925-34.

17. Sonnleitner ST, Sonnleitner S, Hinterbichler E, Halbfurter H, Kopecky DBC, Koblmuller S, et al. The mutational dynamics of the SARS-CoV-2 virus in serial passages in vitro. Virol Sin. 2022;37(2):198-207.

18. Lei C, Yang J, Hu J, Sun X. On the Calculation of TCID(50) for Quantitation of Virus Infectivity. Virol Sin. 2021;36(1):141-4.

19. Garrison EPMG. Haplotype-based variant detection from short-read sequencing. arXiv. 2012.

20. Li H. Aligning sequence reads, clone sequences and assembly contigs with BWA-MEM. arXiv. 2013.

21. McLaren W, Gil L, Hunt SE, Riat HS, Ritchie GR, Thormann A, et al. The Ensembl Variant Effect Predictor. Genome Biol. 2016;17(1):122.

22. Kent WJ, Sugnet CW, Furey TS, Roskin KM, Pringle TH, Zahler AM, et al. The human genome browser at UCSC. Genome Res. 2002;12(6):996-1006.

23. Tonkin-Hill G, Martincorena I, Amato R, Lawson AR, Gerstung M, Johnston I, et al. Patterns of within-host genetic diversity in SARS-CoV-2. Elife. 2021;10.

24. Turakhia Y, Thornlow B, Hinrichs A, McBroome J, Ayala N, Ye C, et al. Pandemic-scale phylogenomics reveals the SARS-CoV-2 recombination landscape. Nature. 2022;609(7929):994-7.

25. Cao Y, Yisimayi A, Jian F, Song W, Xiao T, Wang L, et al. BA.2.12.1, BA.4 and BA.5 escape antibodies elicited by Omicron infection. Nature. 2022;608(7923):593-602.

26. Johnson BA, Xie X, Bailey AL, Kalveram B, Lokugamage KG, Muruato A, et al. Loss of furin cleavage site attenuates SARS-CoV-2 pathogenesis. Nature. 2021;591(7849):293-9.

27. Tada T, Dcosta BM, Samanovic MI, Herati RS, Cornelius A, Zhou H, et al. Convalescent-Phase Sera and Vaccine-Elicited Antibodies Largely Maintain Neutralizing Titer against Global SARS-CoV-2 Variant Spikes. mBio. 2021;12(3):e0069621.

28. Dupont L, Snell LB, Graham C, Seow J, Merrick B, Lechmere T, et al. Neutralizing antibody activity in convalescent sera from infection in humans with SARS-CoV-2 and variants of concern. Nat Microbiol. 2021;6(11):1433-42.

29. Tarres-Freixas F, Trinite B, Pons-Grifols A, Romero-Durana M, Riveira-Munoz E, Avila-Nieto C, et al. Heterogeneous Infectivity and Pathogenesis of SARS-CoV-2 Variants Beta, Delta and Omicron in Transgenic K18-hACE2 and Wildtype Mice. Front Microbiol. 2022;13:840757.

30. Rahimi F, Talebi Bezmin Abadi A. Implications of the Emergence of a New Variant of SARS-CoV-2, VUI-202012/01. Arch Med Res. 2021;52(5):569-71.

31. Sedova M, Jaroszewski L, Iyer M, Godzik A. Monitoring for SARS-CoV-2 drug resistance mutations in broad viral populations. bioRxiv. 2022.

32. Kandeel M, Abdelrahman AHM, Oh-Hashi K, Ibrahim A, Venugopala KN, Morsy MA, et al. Repurposing of FDA-approved antivirals, antibiotics, anthelmintics, antioxidants, and cell protectives against SARS-CoV-2 papain-like protease. J Biomol Struct Dyn. 2021;39(14):5129-36.

33. Hammond J, Leister-Tebbe H, Gardner A, Abreu P, Bao W, Wisemandle W, et al. Oral Nirmatrelvir for High-Risk, Nonhospitalized Adults with Covid-19. N Engl J Med. 2022;386(15):1397-408.

34. Pastorio C, Zech F, Noettger S, Jung C, Jacob T, Sanderson T, et al. Determinants of Spike infectivity, processing, and neutralization in SARS-CoV-2 Omicron subvariants BA.1 and BA.2. Cell Host Microbe. 2022;30(9):1255-68 e5.

35. Zeng C, Evans JP, Faraone JN, Qu P, Zheng YM, Saif L, et al. Neutralization of SARS-CoV-2 Variants of Concern Harboring Q677H. mBio. 2021;12(5):e0251021.

36. Kim K, Calabrese P, Wang S, Qin C, Rao Y, Feng P, et al. The roles of APOBEC-mediated RNA editing in SARS-CoV-2 mutations, replication and fitness. Sci Rep. 2022;12(1):14972.

Figures:

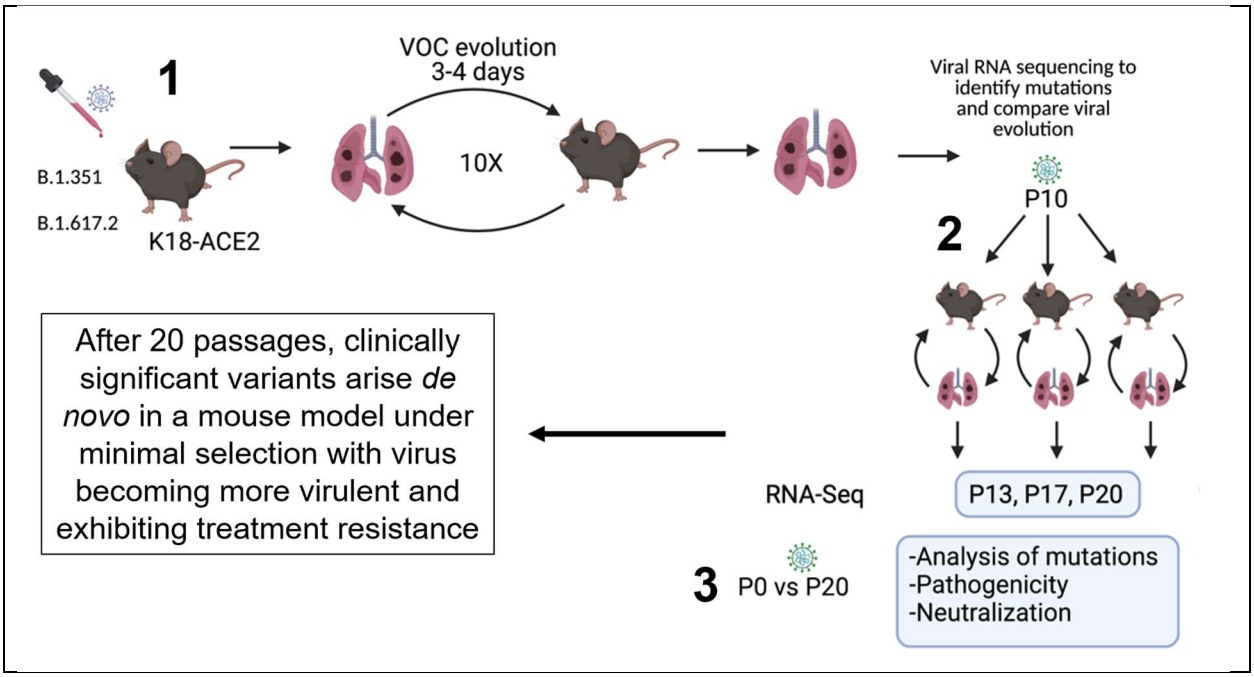

Figure 1. **Study design**. First, SARS-CoV-2 ACE2-adapted mice were inoculated with either B.1.351 (Beta) or B.1.617.2 (Delta) virus and left for three days for virus to proliferate. They were then sacrificed with the lung homogenate used to infect another mouse. This was repeated for ten passages. Second, P10 virus for each lineage was used to infect three additional mice and the process was repeated for an additional ten passages. Third, P0 and P20 virus for each lineage was used to infect additional mice to compare weight loss and survival between early and late passage virus, and test non-adapted mouse susceptibility to the virus. Antibody neutralization of virus was also compared.

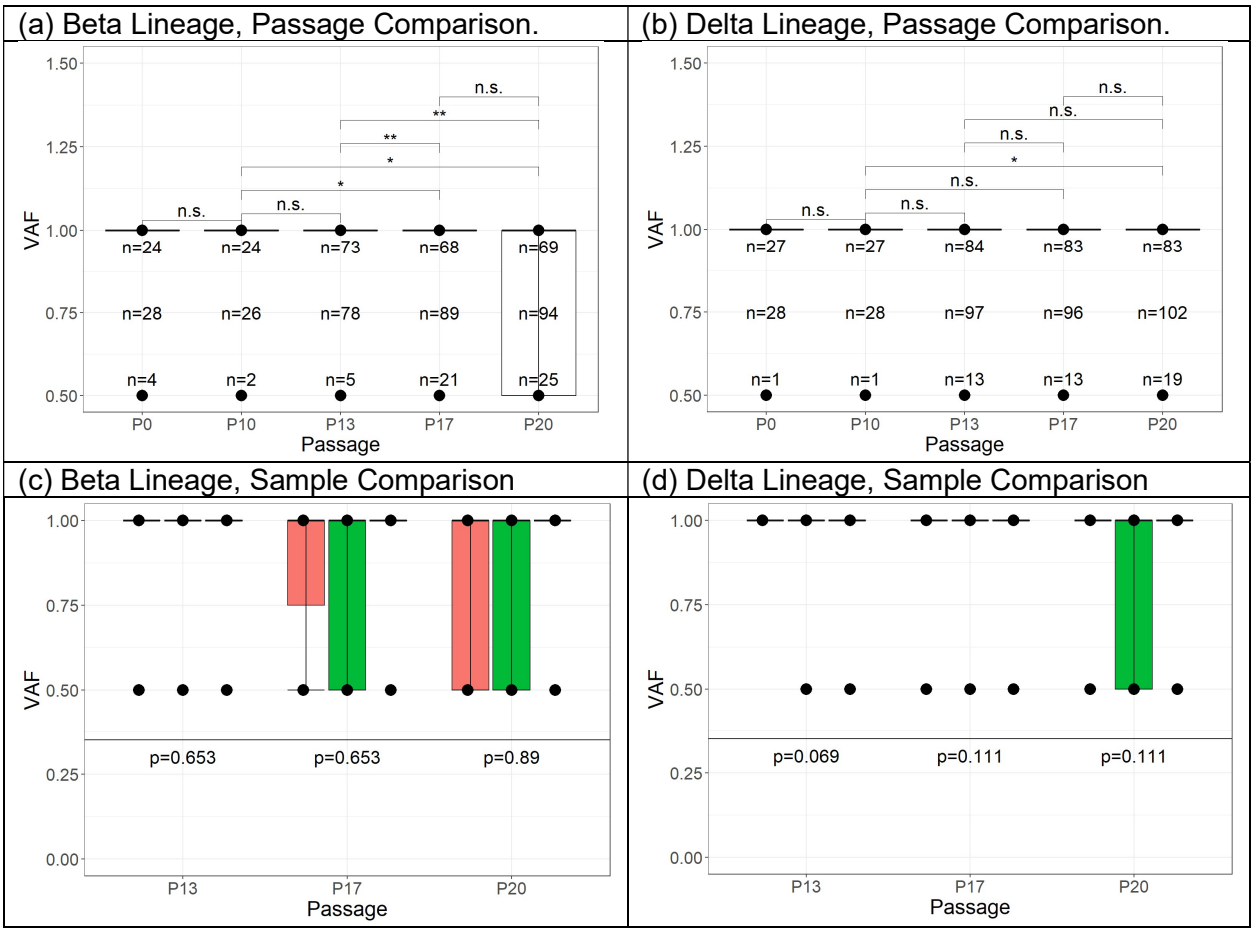

Figure 2. Boxplots of variant allele frequency by (a-b) passage and (c-d) sample. Each N refers to the number of variant alleles for each MAF and in total. Box fill in (c-d) signifies sample number. For significance, n.s.: adjusted p-value > 0.05, *: adjusted p-value > 0.01, **: adjusted p-value ≤ 0.01.

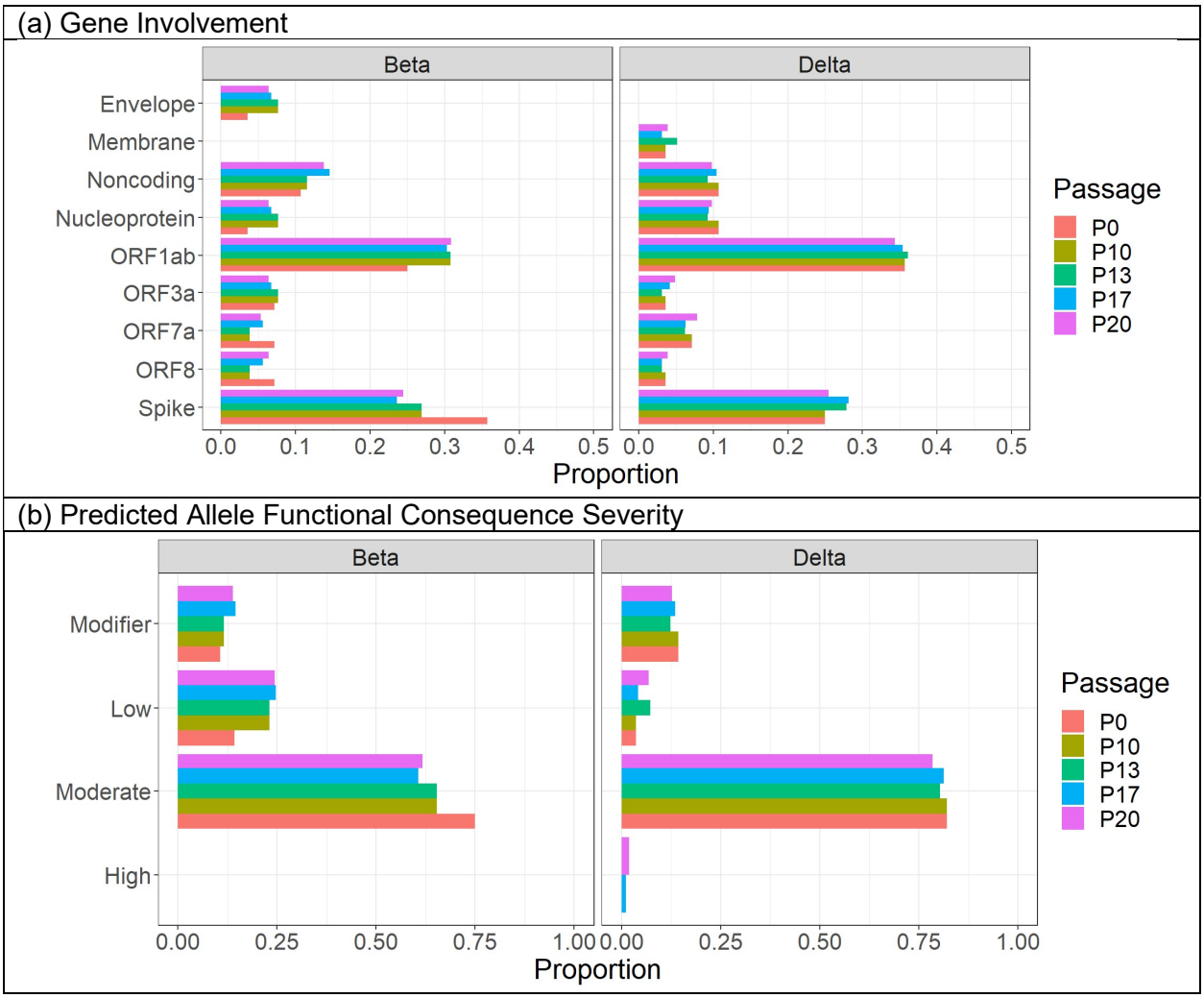

Figure 3. **Gene involvement and predicted variant allele functional consequence severity (VEP) in variant allele population did not significantly change (adjusted p-value > 0.05) with passage.**

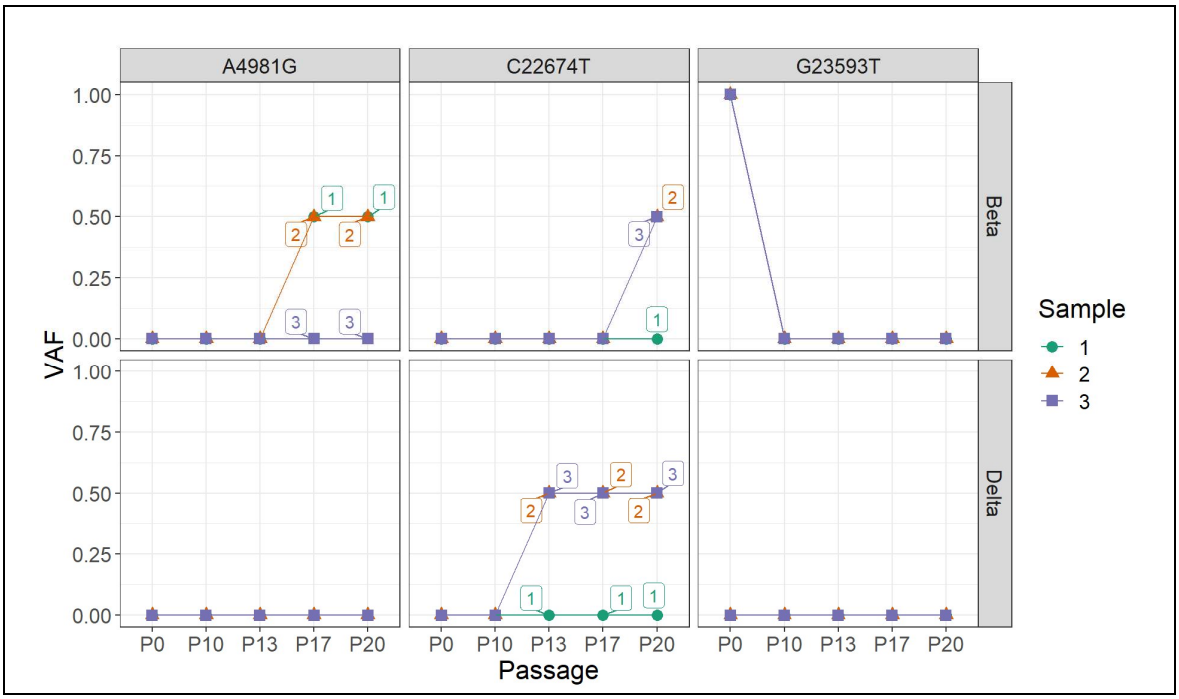

Figure 4. Variants of clinical relevance arose de novo and grew to dominance. VAF: variant allele frequency. P refers to passage.

Variant	Amino Acid Change	Annotation
A4981G	ORF1ab T1572T	Mutations that may confer drug resistance[1]
C22674T	Spike S371F	Protein interacting, antibody escape, vaccine target, Omicron-associated variant allele[1]
G23593T	Spike Q677H	Protein interacting, vaccine target[1], enhances treatment resistance[2], increases infectivity[2]

Table 1. Annotations of select variants that changed in frequency across the study.

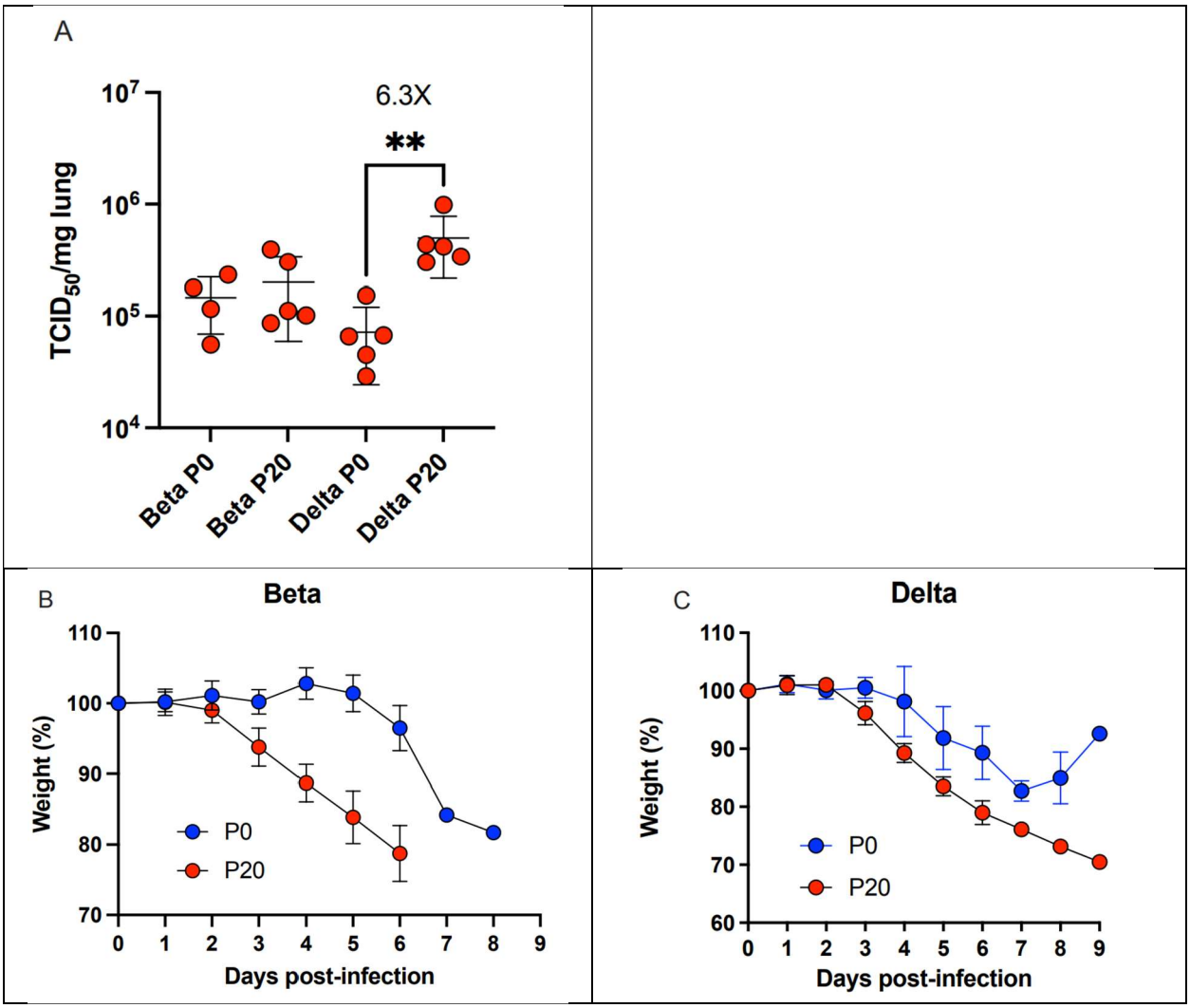

Figure 5. Pathogenesis of P0 and P20 viruses in K18-ACE2 mice. Mice (n = 15/group) were infected with 500 $TCID_{50}$ of P0 or P20 Beta and Delta viruses. (A) On day 3 post-infection, mice (n = 5) were euthanized and lungs collected for infectious viral load determination. Results are expressed as mean ± SD SARS-CoV-2 $TCID_{50}$/mg of lung tissue. (B-C) The weight of each mouse (n = 10/group) was monitored daily throughout the experiment and reported as mean percentage ± SD of weight relative to day 0. **: $p \leq 0.008$ as determined using non-parametric Mann-Whitney test.

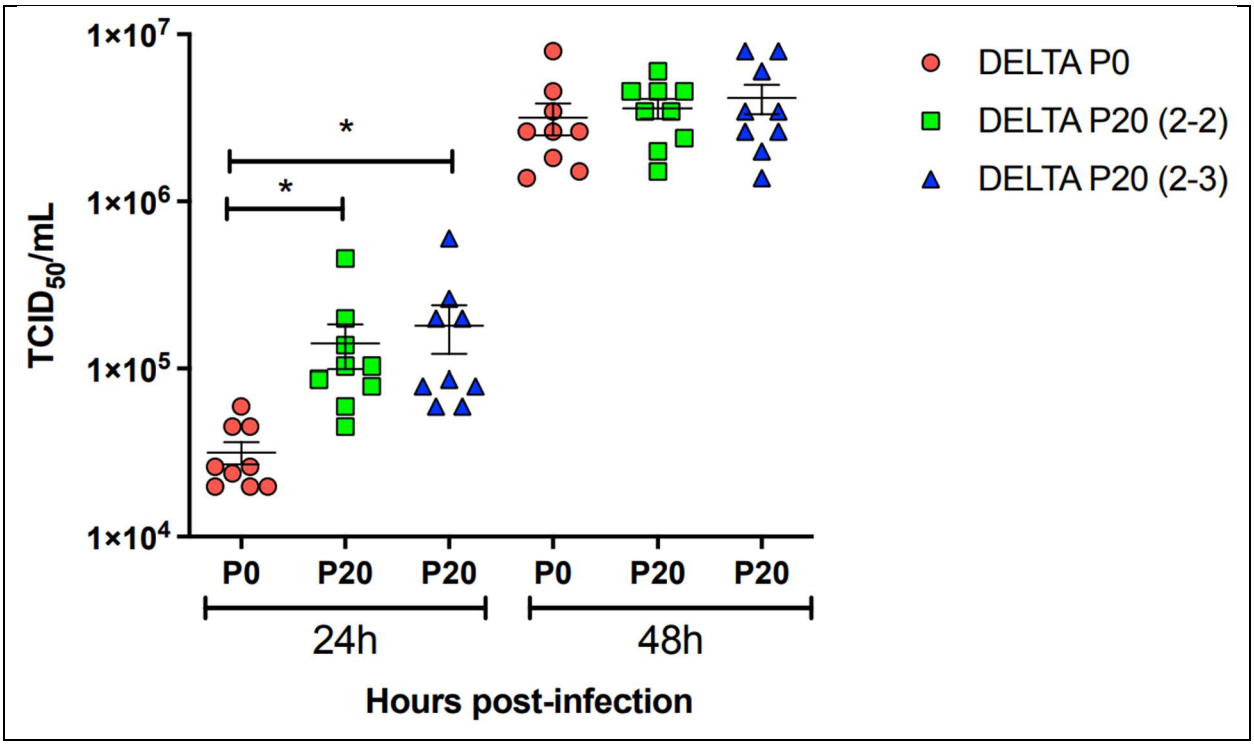

Figure 6. **Growth kinetics of P0 and P20 Delta viruses**. P0 and two independently evolved P20 Delta viruses were used to infect Vero cells at a multiplicity of infection of 0.005. Cell-free supernatants were collected at 24 h and 48 h and used for viral titration. Results are expressed as mean ± SD $TCID_{50}$/mL. *: p=0.02 as determined using an unpaired t-test.

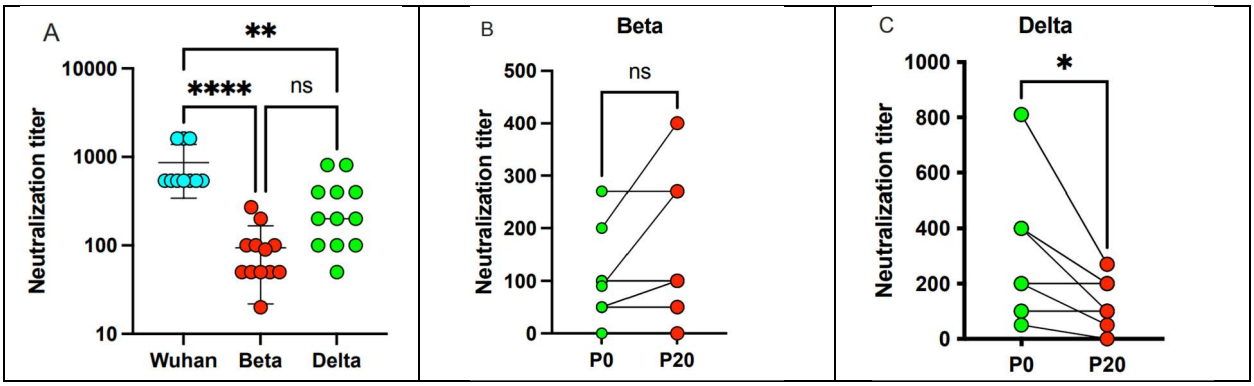

Figure 7. Neutralization of P0 and P20 viruses with sera from vaccinated subjects. (A) Neutralization assay of Wuhan-like, Beta, and Delta viruses using sera from three vaccinated subjects. Individual results and mean ± SD neutralization titer against different SARS-CoV-2 isolates are presented. ****: $p<0.0001$ and **: $p=0.0012$ determined using one way-ANOVA. ns: not statistically significant. (B) Pair-wise comparison of the sera used in A in neutralization assay against P0 and P20 Beta viruses. (C) Pair-wise comparison of the sera used in A in neutralization assay against P0 and P20 Delta viruses. *: $p=0.017$ determined using paired t-test.

Figure References.

1. Kent, W.J., Sugnet, C.W., Furey, T.S., Roskin, K.M., Pringle, T.H., Zahler, A.M., and Haussler, D. (2002). The human genome browser at UCSC. Genome Res *12*, 996-1006. 10.1101/gr.229102.
2. Zeng, C., Evans, J.P., Faraone, J.N., Qu, P., Zheng, Y.M., Saif, L., Oltz, E.M., Lozanski, G., Gumina, R.J., and Liu, S.L. (2021). Neutralization of SARS-CoV-2 Variants of Concern Harboring Q677H. mBio *12*, e0251021. 10.1128/mBio.02510-21.